DUCTILE FRACTURE TOUGHNESS UNDER BIAXIAL LOADING

S Arndt*and A G Atkins†

Cotterell-Mai determinations of the fracture toughness R of 1.6mm thick 5754 ductile aluminium alloy sheets have been made using cruciform testpieces arranged to have the double-edge-notch geometry. Experiments were performed using a novel rig which permits biaxial loadings to be achieved in a uniaxial testing machine. A wide range of in-plane biaxiality ratios λ was employed, including $\lambda<1$ where the loading parallel to the starter ligament was greater than that normal to it. R is somewhat dependent on the remote in-plane biaxiality ratio, greater effects being seen for biaxiality ratios <1. The plane strain necked geometry in which the cracks finally run is little affected by the remote loading. The variation of R with λ is predicted using McClintock/Rice-Tracey models, taking account of the different rates of damage accumulation at the site of fracture before and after neck formation.

INTRODUCTION

Figure 1 shows how different tensile biaxialities are achieved by orientating cruciform testpieces at different angles in a special rig in a uniaxial testing machine. The biaxiality ratio λ is determined by force resolution perpendicular to the axis of the machine, giving $\lambda = \cot\theta$. Thus, a 45° set up produces a 1:1 tensile loading; 30° a 1.73 (perpendicular to the ligament):1 (parallel to the ligament); 60° a 0.59:1 loading. Superimposed bending is minimal as shown by experiments and fem calculations [2]. In the present study we used cruciform testpieces having two cracks along the centre lines of the 'transverse arms' to leave a ligament in the centre of the specimen directly across the line of action of the 'axial' load, Figure 1. We thus have biaxially-loaded 'deep double edge notch' (DENT) specimens which we analysed by the Cotterell-Mai method [3-5]. There are two complementary ways of determining toughness. The essential features of the original test method are (i) to measure the work done U in breaking different length ligaments (the distance L between the ends of the starter cracks); (ii) to plot that work normalised by Lt (where t is the thickness of the sheet) vs L; and (iii) to determine the fracture toughness

* D C White & Partners, Dogmersfield, Hants, RG27 8SX
† Department of Engineering, Reading University, RG6 6AY

from the ordinate intercept of the plot. The straight line plot of (U / Lt) vs L comes about from adding the fracture work (RtL) and the plastic work $(Y\varepsilon)(\pi L^2 t / 4)$ which is confined to a circular patch with ligament as diameter. The effective strain ε in the circular patches is essentially constant for all ligaments, since it is an 'upside-down hardness test'. Y is a mean flow stress. The second method of analysis determines the critical crack opening-displacement (COD, δ_c) by back extrapolation of a plot of the load-point-displacement at final fracture (δ_f) vs L. The theory behind this second method of analysis may be found in Cotterell & Mai [6].

When the ligament breaks under biaxial loading, the load drops. To obtain the work dissipated in fracture, the testpieces are unloaded on the testing machine, to give load-displacement (P - δ) diagrams such as shown in Figure 2. There are, of course, three P - δ diagrams to inspect, viz (i) the testing machine total load versus crosshead displacement (corrected for machine stiffness), and the pair of P - δ diagrams for the loads (ii) across the uncracked ligament and (iii) parallel to the uncracked ligament. Displacement gauges placed along and perpendicular to the uncracked ligament showed that the load-point displacement parallel to the crack essentially ceases at crack propagation (or at necking if that precedes cracking in ductile materials) and that no external work is done in the transverse direction during propagation. Thus the dissipated work U for use in the Cotterell-Mai U/Lt vs L plots, from which the biaxial R are obtained, is that done perpendicular to the uncracked ligament. The work done, in the zone of plasticity around the ligament, by loads parallel to the uncracked ligament before fracture, causes microstructural damage in the region where the crack eventually propagates. The magnitude of this effect depends upon the biaxiality, and hence the fracture toughness R will change with biaxiality.

RESULTS

The Cotterell-Mai U/Lt vs L plots for various remote load biaxialities λ gave good straight line fits. Some are shown in Figure 3. The fracture toughness is given by the y-axis intercept and this varies somewhat with λ. The graphs for $\lambda>1$ all have similar slopes (ca.21MJ/m^3) which represents the remote work/volume performed in the cylindrical zone of plasticity having ligament as diameter. For $\lambda<1$ (where the load parallel to the ligament is greater than that across the ligament), the slopes are progressively steeper, rising to 31MJ/m^3 in the case of the $\theta = 60°$, $\lambda = 0.58{:}1$ ratio. The variation of fracture toughness with λ is shown in Figure 4. Similarly, the load-point displacement at fracture plots linearly against L (Figure 5); as before, the slopes of these graphs have similar values for $\lambda>1$ (ca. 0.14~0.15) but for $\lambda<1$, they increase progressively, becoming 0.27 for the $\theta = 60°$ (0.58:1) orientation. The y-axis intercepts give δ_c, the variation of which with λ is also shown in Figure 4.

DISCUSSION AND CONCLUSIONS

In all our experiments the crack ran 'straight across' in the reduced-thickness 'groove' provided by the neck formed along the ligament. All these results indicated reduced

values of R and δ_c for $\lambda<1$ (Figure 4). Other materials (such as ABS polymer), less ductile than the 5754 alloy, show much less necking and the cracks can turn and climb out of the reduced-thickness necked region and begin to propagate approximately perpendicular to the greater load [7]. Determinations of associated toughness in these cases indicate that crack resistance *increases* above the equibiaxial tension $\lambda = 1$ value; in the 5754 alloy results, the toughness apparently *decreases* below the equibiaxial tension value. It follows that the degree of necking and crack path direction can influence the resistance to cracking.

It is possible to make McClintock/Rice-Tracey predictions for the variation of R and δ_c with λ [7], as shown in Figure 6. The plots depend upon $\bar{\varepsilon}_o$ (the strain at which voiding starts) and whether $\bar{\varepsilon}_o$ is biaxial dependent. Figure 6 has been calculated for $\bar{\varepsilon}_o = 0$ and while the theoretical plots take the right sort of shape, quantitative agreement is not good for $\lambda>1$ where the theory predicts a much more gradual $dR/d\lambda$ and $d\delta_c/d\lambda$ than observed. It may be shown that better predictions are obtained when $\bar{\varepsilon}_o$ reduces as the hydrostatic stress σ_H increases [8-10].

REFERENCES

[1] Anon., Flight, 1919.

[2] Barber, A.G., Univ. Reading, Dept Engineering Final Year Project, 1991.

[3] Cotterell, B. and Reddell, J.K., Int. J. Fract. Vol. 13, 1977, pp267-273.

[4] Cotterell, B. and Mai, Y.W., Int. J. Fract. Vol. 24, 1984, pp229-240.

[5] Cotterell, B., Lee, E. and Mai, Y.W., Int. J. Fract. Vol. 20, 1982, pp243-252.

[6] Cotterell, B. and Mai, Y.W., Proc. ICF-5. Vol. 4, 1982, pp1683-1684.

[7] Atkins, A.G., Jeronimidis, G. and Arndt, S., J. Mater. Sci (in press), 1998.

[8] LeRoy, G., Emburey, J.D., Edwards, G. and Ashby, M.F., Acta. Metall. Vol 29, 1981, pp1509-1521.

[9] Atkins, A.G., Irwin Festschrift (Rossmanith, P., Ed). Amsterdam, Balkema, 1997, pp327-350.

[10] Atkins, A.G. and Mai, Y.W., 'Elastic & Plastic Fracture'. Chichester: Ellis Horwood, 1985 and 1988.

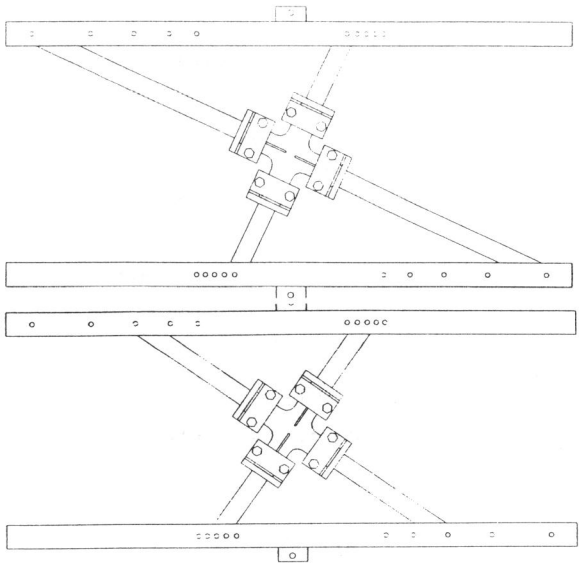

Figure 1 Cruciform rig set at θ = 25° (top) and 55° (bottom)

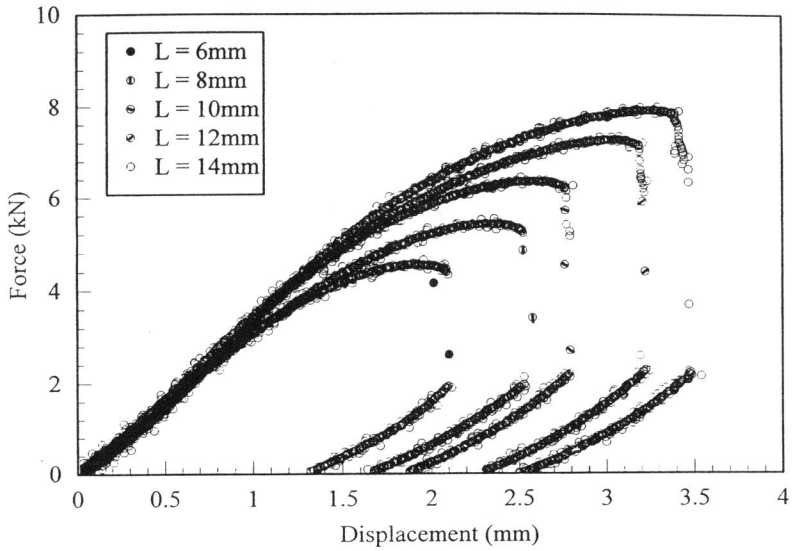

Figure 2 Force-deflexion plots for cruciform specimens at θ = 35° for various ligament lengths

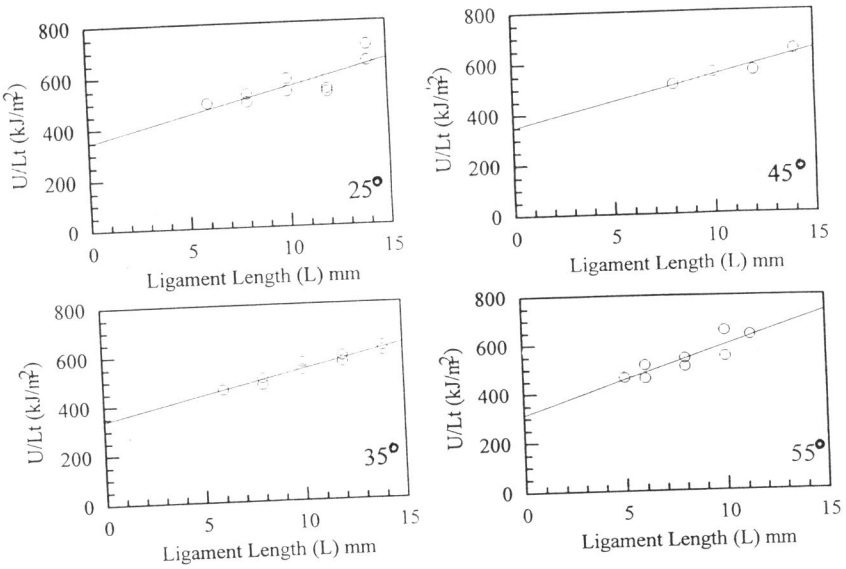

Figure 3 Normalised work of fracture plots at various rig orientations θ.

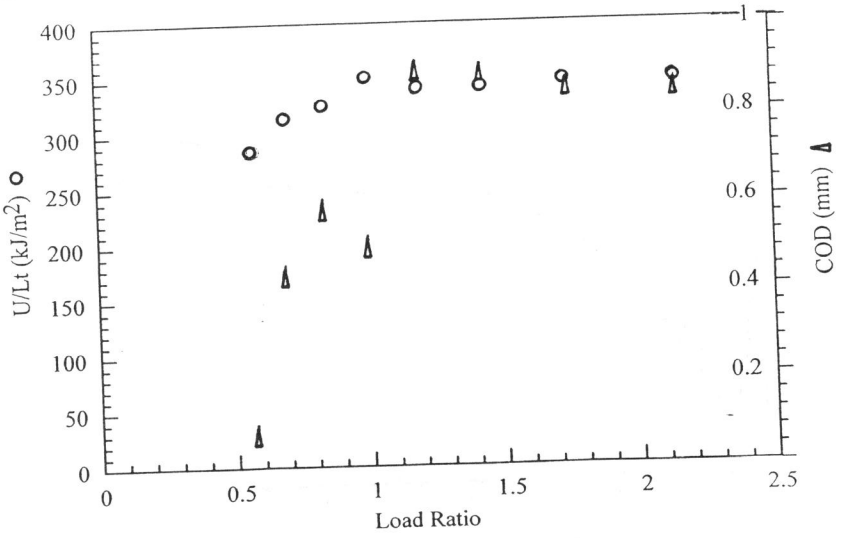

Figure 4 Plots of fracture toughness R(o) and COD(Δ)

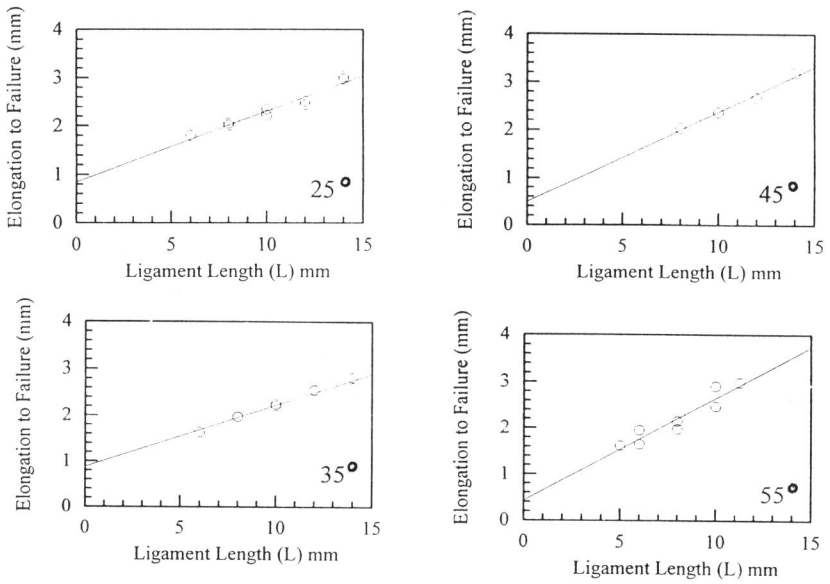

Figure 5 Load-line displacement-at-fracture plots at various rig orientations

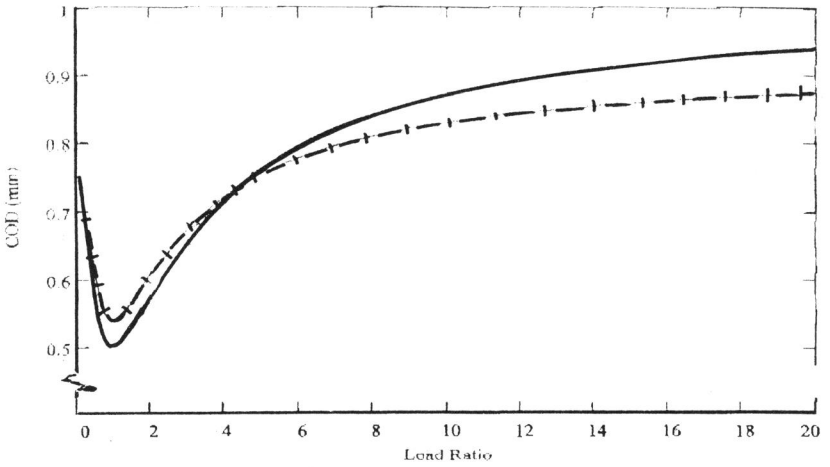

Figure 6 McClintock(-)/Rice-Tracey(+) predictions of COD vs λ $\left(\bar{\varepsilon}_o = 0\right)$